Applied Geochemistry 119 (2020) 104610

Contents lists available at ScienceDirect

Applied Geochemistry

journal homepage: http://www.elsevier.com/locate/apgeochem

The effect of water exchange on the leaching of alum shale

Froeydis Meen Waersted (Frøydis Wærsted)[a,*], Patrick Johannes Riss (Riß)[b], Lindis Skipperud[a]

[a] Centre for Environmental Radioactivity (CERAD), Faculty of Environmental Sciences and Natural Resource Management, Norwegian University of Life Sciences, P.O. Box 5003, N-1432, Ås, Norway

[b] Department of Chemistry, Faculty for Mathematics and Natural Sciences, University of Oslo, Sem Sælands vei 26, N-0371, Oslo, Norway

ARTICLE INFO

Editorial handling by Prof. M. Kersten

Keywords:
Alum/black shale
Acid/neutral rock drainage
Naturally occurring radioactive materials (NORM)
Trace elements

ABSTRACT

In recent years, there has been an increasing focus on the adverse environmental effects from naturally occurring radioactive materials (NORM). Acid rock drainage (ARD) produced by debris from mining and construction work is a major environmental issue, leading to release of highly acidic water as well as both NORM and stable trace elements. Batch leaching experiments with alum shale demonstrated that exchange of water will increase leaching of elements whose mobility is limited by concentration effects, such as Ba and the extremely radiotoxic, naturally occurring uranium daughter ^{226}Ra. Periods of drying the alum shale in air increased leaching of Li, V, Mo and ^{226}Ra, increasing their mobility in the environment. Acid production from sulphide oxidation did not cause pH values below 6.4 in the 28 weeks experiment. However, exchange of water did lead to reduction of inherent buffer capacity of the alum shale, which increases the risk of ARD as well as likely reducing the time before onset of ARD.

1. Introduction

Today, the global population growth and increasing rate of consumption cause rising demands for raw materials. Many of these raw materials are mined, which often has major environmental consequences. Rock debris from mining or construction work in certain geological areas can be a major source of naturally occurring radioactive material (NORM) and stable trace elements. Storage conditions for such debris are critical for weathering rates and consequently influence the release of contaminants into the environment. Certain types of rock produce acid when exposed to air and water, which in itself can be detrimental to the downstream environment and also greatly enhances release and mobility of a range of elements in a phenomenon termed *acid rock drainage* (ARD) (Appelo and Postma, 2010; vanLoon and Duffy, 2011).

Alum shale is a sedimentary, Cambro-Ordovician black shale (black mudrock) formed under reducing conditions. Black shales are found throughout the world, with particularly large deposits in Northern Europe as well as Russia, North America, Australia, China and Brazil (Alloway, 2013). Alum shale contains silicate minerals, sulphides, carbonates and organic matter (kerogen), and is enriched with several trace elements including Ba, V, Mo, Co, Ni, Cu, Zn, Cd, and As, as well as the uranium-series (Falk et al., 2006; Owen et al., 1990; Pabst et al., 2016). The primordial radionuclide ^{238}U in unweathered alum shale is in secular equilibrium with highly radiotoxic daughter nuclides such as ^{226}Ra, i.e. these daughters are present in the same activity as ^{238}U. As alum shale is excavated and weathering processes start, sulphide minerals (like pyrite and pyrrhotite) in the alum shale can be oxidized, causing production of acid. Carbonates in the rock (such as calcite) can neutralize the acid. Consequently, the ratio of the (acid) neutralization potential (NP) to the acidification potential (AP) is a very important property of rock masses to consider when choosing conditions for storage (Lawrence and Scheske, 1997; Pabst et al., 2016). Rock masses are considered neutralizing when NP:AP is above 3 and acid-producing when the ratio is below 1, while masses with ratio between 1 and 3 fall into the uncertainty zone.

Improper storage of acid-producing rock debris can be detrimental for the local environment; major costs are associated with remediation of old sites and preventive measures when closing down mines (Parbhakar-Fox and Lottermoser, 2015; Pipkin et al., 2008). Different approaches can be used for storage to avoid negative effects on the environment, and measures can be divided into active and passive categories (Hindar, 2010). Passive measures are often taken to avoid or reduce weathering of the material, and as such eliminate the generation of ARD. To reduce or avoid weathering of the debris, passive measures will have to strictly limit the availability of water and/or oxygen as both are needed for the oxidation of sulphides (Appelo and Postma, 2010). In

* Corresponding author.
E-mail addresses: froydis.meen.warsted@nmbu.no (F.M. Waersted), patrick.riss@kjemi.uio.no (P.J. Riss), lindis.skipperud@nmbu.no (L. Skipperud).

https://doi.org/10.1016/j.apgeochem.2020.104610
Received 25 November 2019; Received in revised form 17 April 2020; Accepted 20 April 2020
Available online 5 May 2020

Abbreviations

AP	Acidification Potential
ARD	Acid Rock Drainage
DL	Detection Limit
DOC	Dissolved Organic Carbon
ICP-MS	Inductively Coupled Plasma Mass Spectrometry
K_{SP}	Solubility Product
LMM	Low Molecular Mass
LOI	Loss On Ignition
NORM	Naturally Occurring Radioactive Material
NP	Neutralization Potential
NRD	Neutral Rock Drainage
OM	Organic Matter
ORP	Oxidation-Reduction Potential
TIC	Total Inorganic Carbon
TOC	Total Organic Carbon
XRD	X-Ray Diffraction

contrast, active measures, such as water treatment, may become necessary when passive measures have failed. Active measures are generally more expensive and require a long-term commitment.

One passive storage option is to submerge the masses in water, and cover the site with a tight top layer to avoid the intrusion of air (Sørmo et al., 2015). The water should remain stagnant as exchange of the liquid phase leads to influx of oxygenated water and release of contaminated water. This requires a completely sealed disposal site. Another passive storage option is to add neutralizing material like shell sand or similar sources of carbonates to the disposal site (Hindar, 2010). While weathering will occur, the added material will neutralize the produced acid and reduce mobility of several trace elements that are more soluble at lower pH (Sørmo et al., 2015). However, even at neutral pH, NORM and stable elements incorporated in the alum shale can be released during oxidation, in a process termed *neutral rock drainage* (NRD) (Alloway, 2013; Appelo and Postma, 2010; Sima et al., 2011).

Avoiding exchange of water and intrusion of air can be difficult when storing rock masses submerged in water, in both short term and long-term perspectives, and even carefully planned disposal sites might not fulfil these criteria. Groundwater levels can fluctuate, and in dry periods masses normally below the groundwater table can be exposed to air. Additionally, debris from older mining and construction work has often been stored without consideration of these issues, and continues to be at multiple sites around the world today (see e.g. Dold, 2017; Falk et al., 2006; Sima et al., 2011; Stegnar et al., 2013).

This study investigates effects from improper storage of acid-producing alum shale using batch leaching experiments with debris from construction work. The effect of exchange of water on the leaching of the contaminants was investigated by cyclic exchange of the leachant. Furthermore, the effect of fluctuating water levels in a disposal site was simulated with cyclic drying and submerging of the debris. Leaching behaviour of 21 elements was investigated. Main constituents of the alum shale (Ca, K, Al, S, Fe, carbonates) were investigated in the leachate to monitor processes occurring in the alum shale debris. Important water quality parameters including pH, main anions and cations, were measured, and trace elements expected to be enriched in alum shale (Ba, V, Mo, Co, Ni, Cu, Zn, Cd, As, ^{238}U and ^{226}Ra) were included to assess potential environmental threats. Additionally, Li, Sr, Mn and Sb were included as literature information about their leaching from alum shale was scarce.

2. Materials and methods

2.1. Materials

2.1.1. Sample description and handling

In Norway, alum shale is mainly found in the Oslo region (Endre and Sørmo, 2015), and comprises horizon 2-3a in the Ordovician succession (Owen et al., 1990; Pabst et al., 2016). The alum shale formation ranges in thickness from about 20 to almost 100 m. The alum shale at Gran has been found to have lower concentrations of sulphides compared to sulphides further south in the Oslo region, but is still expected to be net acid producing (Endre, 2013).

In 2013-2015 a road tunnel was constructed at Gran, Hadeland, Norway (Fig. 1) cutting through the alum shale formation (Fjermestad et al., 2018). Alum shale debris used in this study originates from a tunnel blast in the alum shale formation performed on the May 19, 2015, and was collected on the same day. Handheld XRF (Niton™ XL3t GOLDD+, Thermo Scientific) was used during sampling to ensure that alum shale with high content of U was collected.

Previous geochemical characterization placed the alum shale batch in the 3a layer of the alum shale formation (Wærsted, 2019), by comparing whole-rock analysis data (elemental composition, total inorganic carbon (TIC) and total organic carbon (TOC)) as well as calculated acidification and neutralization potentials with an existing database of mudrocks from the Oslo region (Norway), as described by Pabst et al. (2016). This layer is expected to be acid producing and to have a high content of both NORM (U-series) as well as several stable trace elements of concern (Owen et al., 1990; Pabst et al., 2016).

The alum shale debris was stored for 18 months before starting the experiment. It was desirable to use fresh rock surface for the experiment as the effect of different storage conditions in a disposal site were to be investigated. Thus, the larger rock pieces (approximately 1–2 cm) were selected, crushed with a jaw crusher the day before the experiment, sieved to collect the finer fraction (2 mm mesh size), and stored under nitrogen overnight until the initiation of the experiment. The finer fraction was used as it was observed on site that a substantial part of the debris was finely crushed; thus this fraction has to be used in a realistic worst-case scenario.

2.1.2. Chemicals

All chemicals used throughout the work were analytical grade unless otherwise noted. Type I water (ASTM D1193-91 standard specifications) was used for all applications.

Synthetic rainwater was prepared to match the specifications of rain falling in Hurdal, a meteorological site within a 27 km radius of the alum shale sampling point (Aas et al., 2015). The average ion concentrations and pH of the rainwater in 2010–2014 was used (Table S1).

Fig. 1. Map showing the position of Gran. Modified from www.kartverket.no, reused under Creative Commons Attribution ShareAlike 3.0.

2.2. Experimental setup

Crushed alum shale (180 g) was mixed with synthetic rainwater (1.8 L) in batch experiments. Four replicates were made for each treatment:

Wet-dry cycles (DRY): Samples were exposed to wet and dry periods where the debris was kept alternately in water (3 weeks) and air (2 weeks). The wet period was repeated six times with dry periods in between (Table 1). During the dry periods, the debris dried completely in about 10 days.

Wet-wet cycles (WET): The water of each sample was exchanged every five weeks without drying the debris.

Samples were kept in the dark at 10 °C in open 2 L polypropylene bottles (Nalgene, Thermo Scientific), covered loosely with plastic foil to reduce evaporation and risk of contamination. All samples were mixed by shaking by hand 2-3 times per week. When sampling intervals allowed it, bottles were shaken 48 h before sampling and left standing to let the debris settle. At the end of each wet period, water was carefully lifted off the solids using a peristaltic pump to minimize loss of particles. One sample consisting of pure artificial rainwater (no debris) kept in parallel to each treatment was treated, sampled and analysed in the exact same way to monitor contamination and other unintended effects in the experiment.

Aliquots for analysis of the leachate were withdrawn at 1 h, 24 h, 1 and 3 weeks after starting a cycle (i.e. after mixing debris with fresh synthetic rainwater) for both treatments, and additionally at 5 weeks for the WET samples. The volume withdrawn during sampling accounted for <15% of the total volume in each cycle, and was replaced by synthetic rainwater. Subsamples of the starting material (crushed alum shale) and leached debris (air-dried at the end of the experiment) were characterized as described in section 2.3.

2.3. Chemical analysis

2.3.1. Alum shale analysis

Total element concentrations were determined by inductively coupled plasma mass spectrometry (ICP-MS) after digesting (260 °C, 40 min, Milestone UltraCLAVE) 0.25 g of debris in triplicate with the following acid mixtures: 5 mL HNO_3 (for Li, Ca, Fe and S), 5 mL HNO_3 + 1 mL HF (Mo, Mn, Zn, Cd, As, Sb and U), and 2 mL HNO_3 + 4 mL H_3PO_4 (Na, K, Mg, Sr, Ba, ^{226}Ra, V, Co, Ni and Al). Rh was added as internal standard. Digested samples were diluted to 50 mL. Certified reference materials were digested and measured in parallel to the samples: NIST 2709a San Joaquin Soil and NSC ZC 73007 soil (all three digestions), NIST 2710a Montana I soil (only HNO_3 digestion), and NSC DC 73325 soil (only HF digestion). When determining ^{226}Ra content, reference materials IAEA-314 (sediment) and IAEA-448 (soil) were used. Results for all reference materials were within the specifications.

The pH (handheld multi-meter, Multi series, WTW) was measured in a 1 + 2 V/V mix of debris and water left overnight. Organic matter (OM) was estimated from loss on ignition (LOI, 550 °C, overnight). Total inorganic (TIC) and organic (TOC) carbon contents in the debris were determined by coulometry. TOC was only measured in the starting material. Particle size distribution was determined for a 10 g sample, where OM had been removed by heating with H2O2, by wet sieving through 0.06 mm (sand fraction) and separating silt and clay (<0.002 mm) by sedimentation according to Stokes' law. Mineral composition was determined by powder X-ray diffraction (XRD) on a D8 Discover (Bruker). The XRD diffractograms were analysed with TOPAS software to identify the peaks using a reference spectra library, and quantified by the Rietveld refinement technique.

2.3.2. Leachate analysis

Leachate aliquots were collected using a syringe, and divided into different subsamples. Conductivity, pH and oxidation-reduction potential (ORP) were measured immediately after sampling on untreated aliquots (handheld multi-meter, Multi series, WTW). E_h was calculated from ORP according to instructions from the manufacturer. Samples for alkalinity, ICP-MS, dissolved organic carbon (DOC) and anion chromatography were immediately filtered through 0.45 μm polyethersulfone membrane syringe filters (VWR), and subsamples for analysis of low molecular mass (LMM) components by ICP-MS were also filtered through 10 kDa Amicon® Ultra-15 centrifugal filters (Merck Millipore). The samples were stored in the dark at 4 °C. Alkalinity was measured by colorimetry by titration to pH 4.5 (ISO 9963–1:1994). Samples for ICP-MS were acidified with 5% (V/V) ultrapure HNO_3. Anions were quantified by ion chromatography (Lachat IC5000 system, Dionex™ IonPac™ AS22-Fast IC column, Dionex AMMS™ 300 ion suppressor, Thermo Scientific). DOC was determined with a TOC-VCPN analyser (Shimadzu), but all samples were below the detection limit (DL) (1.8 mg L^{-1}).

2.3.3. ICP-MS analysis

Li, Na, K, Mg, Ca, Sr, Ba, V, Mo, Mn, Fe, Co, Ni, Zn, Cd, Al, As, Sb, S and ^{238}U were determined in synthetic rainwater, leachate and digested alum shale with an Agilent 8800 Triple Quadrupole ICP-MS instrument. Ge, In, Ir and Bi were added online as internal standards within the instrument. Alternately, He, O_2 and no gas were used in the collision/reaction chamber to remove interferences. To check the accuracy of the method, an in-house standard covering all measured elements was analysed on each day of analysis.

Leachate and digested alum shale were analysed for ^{226}Ra with an Agilent 8900 Triple Quadrupole ICP-MS (Agilent Technologies), using the method of Wærsted et al. (2018) that utilizes N_2O as reaction gas to eliminate interferences.

2.3.4. Data treatment

The total leached mass of each element was estimated for each sample individually according to the equation below.

$$Percent\ leached = \sum_{n=1}^{6} \frac{mass\ in\ solution\ at\ end\ of\ cycle\ n}{mass\ \ in\ starting\ material}$$

The acidification potential (AP) of the debris was estimated by assuming that all S in the rock comes from sulphides behaving like pyrite, and the neutralization potential (NP) was estimated from the TIC, assuming these carbonates behave like calcite (Lawrence and Wang, 1996; Pabst et al., 2016).

As mentioned, one blank was kept in parallel to each treatment and treated in the same way. There were detectable levels of Zn and Ba in

Table 1
Overview of treatment periods. Vertical lines mark the end of a cycle and addition of new leachant. Grey areas represent the dry periods, and white areas the wet periods. Sampling points are approximately marked by crosses.

	Cycle 1					Cycle 2					Cycle 3					Cycle 4					Cycle 5					Cycle 6			
Week	1	2	3	4	5	6	7	8	9	10	11	12	13	14	15	16	17	18	19	20	21	22	23	24	25	26	27	28	
WET	xxx		x		x	xxx		x		x	xxx		x		x	xxx		x		x	xxx		x		x	xxx		x	
DRY	xxx		x			xxx		x			xxx		x			xxx		x			xxx		x			xxx		x	

Table 2
Mineral content of alum shale debris before and after leaching. All results are in percent of weight.

Treatment	n	Muscovite	Quartz	Pyrite	Calcite	Amorphous material
		%	%	%	%	%
Untreated	1	42	20.8	4.3	1.7	31
WET	4	43 ± 5	22.0 ± 1.2	4.2 ± 0.1	0.5 ± 0.3	31 ± 4
DRY	4	45 ± 1	21.7 ± 0.2	4.2 ± 0.1	0.6 ± 0.4	29 ± 1

these blanks, but the sample concentrations were well above the detection limit (DL, 3 × standard deviation of blank) calculated from these blanks.

All figures and tables show average ± one standard deviation of replicate samples. T-tests were used for finding significant differences between treatments (Miller and Miller, 2005).

3. Results and discussion

3.1. Alum shale characterization

The minerals muscovite ($KAl_2(AlSi_3O_{10})(F, OH)_2$), quartz ($SiO_2$), pyrite ($FeS_2$) and calcite ($CaCO_3$) were detected in the debris by XRD measurements (Table 2), and 31% of the material (by weight) was amorphous. The pyrite concentration is in the low range of what Jeng (1991) found in three unweathered, Norwegian alum shales (4.3–13.3%). The calcite content of the rock decreased to about a third of the starting value in both treatments. No reduction of the content of the other minerals was observed. The debris (crushed, as described in section 2.1.1) consisted mainly of sand-sized particles (90.4%), some silt (8.5%) and very little clay (1.1%).

Table 3
LOI, TIC and pH of alum shale debris used in the experiment.

Treatment	n	LOI (%)	TIC (%)	pH
Untreated	1[a]	12.3	0.22 ± 0.02	7.5
WET	4	12.6 ± 0.2	0.09 ± 0.01	6.6 ± 0.1
DRY	4	12.7 ± 0.2	0.10 ± 0.01	6.7 ± 0.3

[a] For the TIC analysis of the untreated alum shale, n = 2.

The measured TIC (Table 3) corresponded well with carbonate content calculated from calcite content. TIC was reduced to less than half of the original value in both treatments ($p < 0.0009$), supporting the observation of reduced calcite content. The content of TIC and calcite represents the main buffer capacity of the debris, and is reduced by dissolution and consumption by acid. TIC concentrations of both the untreated and treated samples were similar to levels found in other alum shales in Norway, and in the lower range of other Cambro-Ordovician black shales in Norway (Pabst et al., 2016).

The pH of the debris decreased by almost one unit from the starting material to the leached debris for both treatments, likely reflecting acidification via oxidation of sulphides (see also paragraph 3.3.3) and consumption of carbonate content during the experiment. Organic matter (estimated by LOI) did not change in either treatment. It makes up less than half of the amorphous material in the sample, which also did not change. Measured TOC in the starting material was 7.8%, which is quite similar to the estimate from LOI (7.2%).

Estimated AP and NP for the untreated alum shale debris were 100 kg $CaCO_3$ eq t^{-1} and 18 kg $CaCO_3$ eq t^{-1}, respectively. Thus, the NP to AP ratio is 0.18, and the debris is clearly expected to be acid producing.

The concentration of ^{238}U in the debris (Table 4) was higher than 1 kBq kg^{-1}, therefore, the debris may be classified as (low-level) radioactive waste (in Norway) (Strålevernforskriften, 2016). Furthermore, the levels of Cr, Ni, Zn, As and Cd exceeded the Norwegian limits for contaminated ground (Pollution Control Act, 2004). Concentrations of the aforementioned elements and other important elements are presented in Table 4, and fall within the rather wide range of concentrations measured in Scandinavian alum shales (Falk et al., 2006; Jeng, 1991, 1992; Lavergren et al., 2009; Pabst et al., 2016). The measured

Table 4
Total element concentrations of the alum shale debris before leaching, together with percent leached in the two treatments and the ratio of the summed leached mass in the treatments. Data for leachates filtrated through 0.45 μm is used. For all measurements, n = 3.

		Alum shale total concentration		WET	DRY	Ratio
				% leached	% leached	DRY:WET
Group 1 *(Alkali metals)*	Li	32 ± 0.6	mg kg^{-1}	0.98	1.2	1.24****
	Na	3.3 ± 0.2	g kg^{-1}	2.3	2.4	1.03**
	K	39 ± 3	g kg^{-1}	0.32	0.35	1.09****
Group 2 *(Alkaline earth metals)*	Mg	9.2 ± 0.4	g kg^{-1}	2.0	2.1	1.05****
	Ca	8.8 ± 2.3	g kg^{-1}	26	25	0.96***
	Sr	182 ± 77	mg kg^{-1}	22	21	0.99
	Ba	656 ± 38	mg kg^{-1}	0.38	0.36	0.96**
	^{226}Ra	30 ± 6	ng kg^{-1}	0.63	0.76	1.22**
		1.1 ± 0.2	kBq kg^{-1}			
Group 4-11 *(Transition metals)*	V	2.9 ± 0.2	g kg^{-1}	0.00097	0.0013	1.38****
	Mo	265 ± 4	mg kg^{-1}	14	18	1.28****
	Mn	311 ± 12	mg kg^{-1}	8.9	8.6	0.96**
	Fe	33 ± 4	g kg^{-1}	<DL	<DL	
	Co	22 ± 2	mg kg^{-1}	1.59	1.64	1.03*
	Ni	366 ± 27	mg kg^{-1}	2.6	2.5	0.98
Group 12 *(Zinc group)*	Zn	564 ± 112	mg kg^{-1}	1.1	1.2	1.07*
	Cd	12 ± 2	mg kg^{-1}	4.0	4.4	1.10***
Group 13 *(Icosagens)*	Al	77 ± 4	g kg^{-1}	0.00025	0.00026	1.06
Group 15 *(Pnictogens)*	As	81 ± 1	mg kg^{-1}	0.018	0.019	1.02
	Sb	20 ± 0.4	mg kg^{-1}	1.7	1.3	0.76****
Group 16 *(Chalcogens)*	S	32 ± 4	g kg^{-1}	4.4	5.0	1.14****
Actinides	^{238}U	110 ± 3	mg kg^{-1}	3.0	2.2	0.71****
		1.37 ± 0.03	kBq kg^{-1}			

Significance levels for *t*-test testing the difference between % leached in WET and DRY treatments: *p < 0.1, **p < 0.05, ***p < 0.01, ****p < 0.001.

muscovite content corresponds well with the K and Al concentrations in the sample. Pyrite contributes 61% of Fe and 72% of S, while 76% of the Ca in the sample is from calcite. The S in the debris that is not accounted for by pyrite can be present both as sulphates and as other sulphides (e.g. pyrrhotite or sulphides with other cations than Fe), either in amorphous forms or in too low concentration to be detected by the XRD measurements. As the calculations for estimating AP assume that all S in the debris is present as sulphides behaving like pyrite, the presence of S as sulphates would mean that the AP has been overestimated to some extent. However, as the environmental consequences of underestimating the AP are far greater than overestimating it, total S is commonly used for the estimation (Dold, 2017). Using e.g. pyrite for the calculations could exclude other acid-producing sulphides like pyrrhotite.

Activity concentration of ^{226}Ra estimated from secular equilibrium with U (1.37 ± 0.03 kBq kg^{-1}) is a bit higher than the measured activity concentration. This is likely caused by one of the three samples for the ^{226}Ra measurements being substantially lower than the other two, reflecting the heterogeneity of the rock debris. The heterogeneity is also reflected in the measured Ca concentration, with close to 30% standard deviation, likely due to presence of carbonate nodules in the rock (Fjermestad et al., 2018; Pabst et al., 2016).

3.2. Water quality parameters

Processes in the debris like pyrite oxidation and carbonate dissolution were expected to be determining factors for a range of parameters in the leaching experiments, and were most probably directly responsible for leachate pH. The lowest measured pH value in the duration of the experiment was 6.5 (Fig. 2 a), and pH was about 7.7 at the end of all cycles. This reflects that calcite was still available for acid neutralization at the end of the last cycle. In the first cycle, pH increased from 5.0 in the artificial rainwater to about 8.0 at 1 h. Then, a sudden drop to 7.4 at 24 h was observed, before pH increased again to 7.8–7.9. This behaviour was also seen by Wærsted (2019), and might be caused by precipitation of Fe (oxy)hydroxides ($FeO_x(OH)_y$) from pyrite oxidation, removing OH^- from solution. Similar curves at somewhat lower pH values were seen for later cycles. The pH in the DRY treatment seemed to be a bit lower than pH in the WET treatment, especially at the beginning of the cycles. In the last cycle the pH values in the two treatments was quite similar.

E_h values measured in the leachate varied from 360 to 490 mV, with no marked differences between the two treatments. Together with the measured pH values, this places the experiment conditions within the stability range of Fe^{III} and $S^{VI}O^{-II}_4{}^{2-}$, and oxidation of pyrite ($Fe^{II}S^{-I}_2$) was, thus, expected (Appelo and Postma, 2010; Grundl et al., 2011).

Conductivity reflects the total amount of ions in the leachate, and, thus, gives an indication about the total leaching from the debris to the aqueous phase for each treatment. The increase in conductivity was faster in DRY than in WET for cycles 2-6 (Fig. 2 b), indicating that the drying period caused oxidation of the debris which lead to a higher release rate of elements. However, due to the longer contact period in the WET treatment, the difference between the two treatments were evened out and in total the DRY treatment was just 2% higher than the WET treatment ($p = 0.03$).

Alkalinity is a measure of the buffer capacity of aqueous solutions, and will, in this case, mainly reflect dissolved carbonates from the calcite. Alkalinity gradually decreased from cycle to cycle in the WET treatment, while for the DRY treatment, the alkalinity in cycle 2 was less than half of that in cycle 1, and leachates in following cycles all reached about the same levels (~0.5 mmol L^{-1}) (Fig. 2 c). Similar trends were seen for pH. Summing the measured alkalinity at the end of each cycle gives a total of 29% less buffer capacity in the DRY leachates compared to the WET ($p < 0.0001$). While the longer contact time in the WET treatment gave more time for dissolution of calcite, the changes in calcite and TIC content of the debris were about the same for both treatments, thus, the difference in measured alkalinity was likely caused by greater sulphide oxidation in the DRY treatment. In 180 g of starting material, there was 33 mmol of carbonate (estimated from TIC). Looking at TIC concentrations in the debris after leaching, it was found that 19 mmol of carbonates were missing in the WET treatment and 18 mmol in the DRY treatment. At the measured pH, aqueous carbonates will mainly be present as HCO_3^-. Assuming that the measured alkalinity represented only carbonates, the carbonates in the leachates at the end of each cycle added up to 9.0 mmol in the WET treatment and 6.4 mmol in the DRY. This represents the fraction of the debris buffer capacity that has simply been removed by changing the leachant, without contributing to acid neutralization. This is a substantial loss of buffer capacity, and was greater in the WET treatment than in the DRY treatment, likely because of greater acid production and carbonate consumption in the DRY treatment. The difference between the carbonates found as alkalinity and the missing carbonates in the leached debris of the two treatments

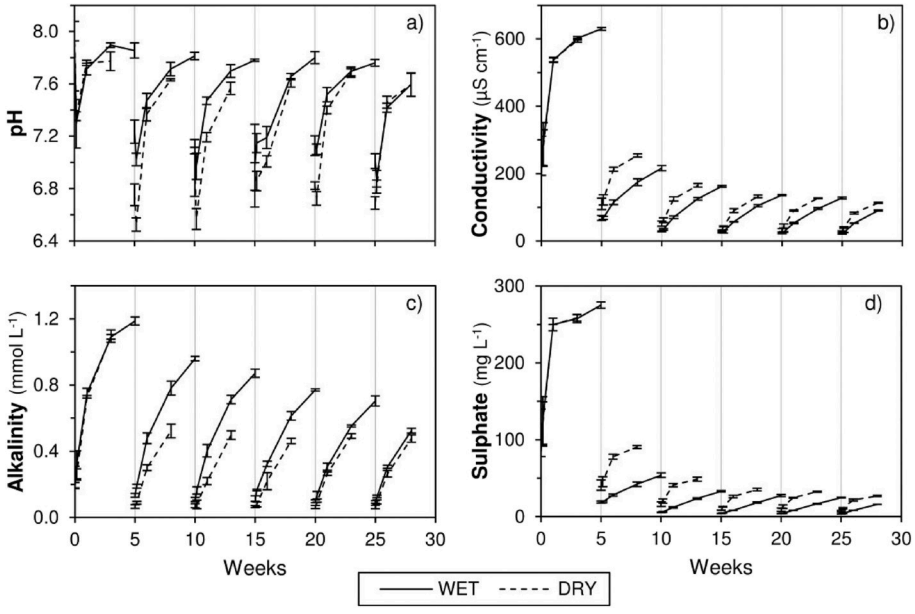

Fig. 2. Changes in water quality parameters with time in the cyclic leaching experiment. Each vertical line represents the start of a new cycle. Full (WET) and dashed (DRY) lines are connecting average concentrations of samples. The error bars represent one standard deviation of replicate samples. For all sampling points, n = 4.

can be assumed to have been consumed by acid neutralization.

Sulphate concentrations increased more rapidly in the DRY compared to the WET treatment in cycles 2-6 (Fig. 2 d). In line with the alkalinity results, this suggests that oxidation of sulphides happened to a larger extent in the DRY samples. This was also expected due to the greater oxygen access in the drying period. In cycles 2-6, sulphate was about twice as high in the DRY treatment compared to the WET at the same time points. The sum of leached sulphate in the whole experiment was 14% higher in DRY compared to WET ($p = 5e\text{-}6$).

Leachate concentrations of Cl^-, NO_3^- and F^- (Figs. S1–S3) were negligible compared to SO_4^{2-}. Cl^- did not change much from the concentration of the synthetic rainwater (Table S1). Concentrations of NO_3^- decreased in each cycle from the concentration of the synthetic rainwater (1.31 mg L^{-1}), possibly indicating biological activity in the samples as NO_3^- is an important nutrient. The reduction was greatest in the first cycles, and in the last cycles there was about 0.5 mg L^{-1} left at the end of the cycles. Concentrations of F^- increased from <DL (0.04 mg L^{-1}) in the synthetic rainwater to about 0.3 mg L^{-1} in the first cycle, then lower concentrations were observed for each cycle and about 0.05 mg L^{-1} in the last cycle. The F^- might originate from the muscovite.

Overall, the measurements of pH, conductivity, alkalinity and sulphate in the leachate all support the initial expectations of greater oxidation rate of sulphides in the DRY treatment compared to the WET, but differences between the treatments seemed to be greatest in cycle 2 and then get smaller for each cycle.

3.3. Leaching of elements over time

All elements leached most rapidly in the first part of the first cycle, likely an artefact resulting from crushing of the rock as hypothesized by Yu et al. (2014). Only for Ba similar leaching rates were observed in later cycles. For most elements, there were statistically significant differences between treatments (see Table 4), even where actual differences were very small and likely not of any practical or environmental implications. Most elements leached more in the DRY treatment despite shorter contact time with the leachant, thus supporting the expectation of greater oxidation in the DRY treatment due to direct contact with air. The higher release rate of an element in the DRY treatment indicates that this element is released from a rock phase directly or indirectly affected by the drying period, e.g., by increased oxidation. The only elements that leached considerably slower in DRY compared to WET were Sb and U (see paragraphs 3.3.4 and 3.3.5). The greatest leaching relative to debris content over the course of the experiments was observed for alkaline earth metals Sr and Ca (21-26%), and transition metals Mn and Mo (8.6–18%) (Table 4). Na, Mg, Co, Ni, Zn, Cd, Sb, S and U leached a few percent of the debris content and the remaining elements <1%.

Results for selected elements are presented in more detail in the following sections, while leaching graphs for other elements can be found in the supplementary information.

3.3.1. Alkali metals

The alkali metals Li, Na and K were all released rapidly within the first week of the first cycle, after which the release rate decreased. In the first cycle, K reached about 5.5 mg L^{-1}, and then leached to lower and lower concentrations in the following cycles (Fig. 3 a). Leaching rates in cycles 2-6 were higher in DRY than in WET, and in the end 9% more leached in the DRY treatment compared to the WET treatment ($p = 6 \times 10^{-7}$). Leaching behaviour of Li (Fig. S4) was very similar to K, though with maximum concentrations of 24 µg L^{-1}. Overall, 24% more Li leached in the DRY treatment compared to the WET ($p = 10^{-6}$). Thus, Li and K seem to originate from rock phases that are affected by the increased oxidation in the drying period. All K in the debris can be accounted for by muscovite, which is not expected to weather before pH drops considerably. However, as only ~0.3% of K was released in the

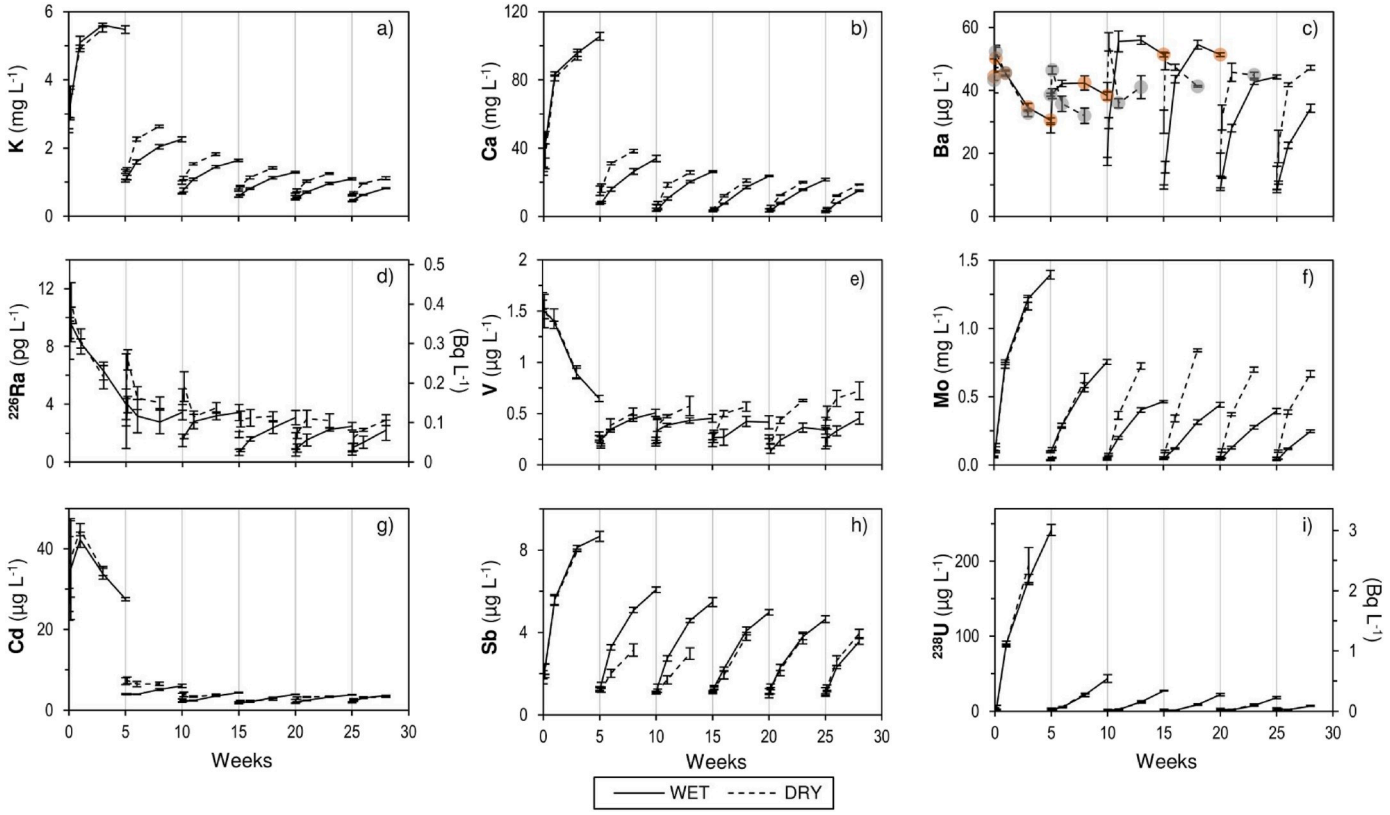

Fig. 3. Dissolved (0.45 µm) concentrations of selected elements as a function of time in the cyclic leaching experiment. Each vertical line represents the start of a new cycle. Full (WET) and dashed (DRY) lines are connecting average concentrations of samples. The error bars represent one standard deviation of replicate samples. For all sampling points, n = 4. In figure c), grey (DRY) and orange (WET) circles mark the sampling points were K_{SP} for $BaSO_4$ is exceeded.

experiment, it could also be originating from a phase that was not detected by XRD.

In the first cycle, Na (Fig. S5) concentrations in both treatments reached about the same concentrations as K. In the second cycle there was some release of Na (0.8–0.9 mg L^{-1}), while in later cycles the concentrations barely exceeded the concentration of the synthetic rainwater used as leachant (0.32 mg L^{-1}). Over the course of the experiment, 3% more Na leached in the DRY than in the WET phase ($p = 0.01$).

3.3.2. Alkaline earth metals

The lighter alkaline earth metals Mg, Ca and Sr all exhibited similar leaching behaviour – though at different concentrations levels – exemplified by Ca in Fig. 3 b. Leaching rates were highest in the first cycle, but leaching continued in the following cycles. In cycles 2-6, leaching rates were higher in the DRY treatment but the longer contact time in the WET treatment made the total % leached in both treatments quite similar for all three elements. Ca leached to the highest concentrations of the three, with about 100 mg L^{-1} in the first cycle and 19-38 mg L^{-1} at the end of the following cycles. Mg reached just above 12 mg L^{-1} in the first cycle and about 1–3 mg L^{-1} in the remaining cycles, while for Sr these numbers were about 2 mg L^{-1} and 0.2–0.7 mg L^{-1}, respectively. Mg leached only about 2% of the total debris content while the other two more than 20%. This could indicate that the fraction of Mg that leached is associated with the same minerals as Ca and Sr, e.g. as replacement for Ca in calcite, which can also be the source of the Sr (Appelo and Postma, 2010; Gabitov et al., 2013), while the main fraction of Mg is bound in a different phase.

Due to the high sulphate concentrations from the pyrite oxidation and dissolution of sulphate minerals, leaching of the heavier alkaline earth metals Ba and ^{226}Ra was expected to be limited by the solubility of $BaSO_4$ and co-precipitation of ^{226}Ra. The peak concentrations of Ba were quite similar in all cycles of both treatments, but the peak appeared at different time points, generally later in the WET compared to the DRY treatment, and later in subsequent cycles (Fig. 3 c), as expected from the observed sulphate concentrations. The points where the solubility product for $BaSO_4$ ($K_{SP} = 1.08 \times 10^{-10}$, 25 °C) (CRC Handbook of Chemistry and Physics, 1993) is exceeded are marked with grey (DRY) and orange (WET) circles in Fig. 3 c. K_{SP} values can be slightly exceeded without precipitation because the conditions in the leachate are different from standard conditions; due to all the other ions in solution, the activity coefficient of Ba^{2+} and SO_4^{2-} can be below 1. Precipitation of $BaSO_4$ was predicted at all sampling points in the first cycle. For the DRY treatment, this was also the case for all of cycle 2 and the last part of cycles 3-5. In the WET treatment, $BaSO_4$ precipitation is expected in the last part of cycles 2 and 3, as well as in 2 out of 4 replicates at 5 weeks in cycle 4. In cycle 6, neither treatments reached K_{SP}.

Leaching behaviour for ^{226}Ra (Fig. 3 d) was similar to what was observed for Ba, except that ^{226}Ra did not reach the same concentrations in later cycles as measured in cycle 1. Furthermore, the total leached mass of ^{226}Ra was 22% higher in the DRY treatment compared to WET ($p = 0.01$), while Ba leached 4% less in DRY ($p = 0.01$). Almost half of the difference between the total ^{226}Ra leaching in the two treatments can be ascribed to the steep decrease in concentrations in the first cycle, caused by increasing sulphate concentrations and precipitation of $BaSO_4$, resulting in lower concentrations at the end of the first cycle of the WET treatment compared to the DRY treatment. On the other hand, a higher leaching rate of ^{226}Ra in the DRY treatment was observed in later cycles, which was likely an actual effect from the drying. The greater leaching of ^{226}Ra in the DRY treatment is opposite of what is expected from the sulphate concentrations. However, this indicates that ^{226}Ra is present in a phase that is sensitive to oxidation effects. Differences in observed behaviour for ^{226}Ra and Ba could be caused by different source phases in the alum shale or that ^{226}Ra was scavenged by $BaSO_4$. The solubility product for $RaSO_4$ ($K_{SP} = 4.25 \times 10^{-11}$) (Kirby and Salutsky, 1964) was never exceeded and Ra thus was co-precipitated with $BaSO_4$ and not precipitating itself. Both, leached Ba and ^{226}Ra, amounted for less than 1% of the total debris content.

3.3.3. Transition metals and group 12

No significant change in the pyrite content of the debris was observed in either treatment (Table 2), even though the water quality parameters quite clearly indicated pyrite oxidation, and the prevailing conditions (i.e., measured pH and E_h values) also favoured oxidation of pyrite. However, the leached amount of S only accounted for 4.4 and 5.0% of the total S in the debris in the WET and DRY treatment, respectively, and a part of this is likely accounted for by dissolution of sulphate minerals. Thus, only a small fraction of the pyrite may have been oxidized, explaining the lack of significant change in measured mineral content.

While concentrations of Fe in solution were below DL (1 μg L^{-1}) for most of the time, Fe was likely important for processes both in the debris and in the solution. As pyrite is oxidized, Fe^{2+} will be released to solution and oxidized to Fe^{3+}, which has a low solubility at circumneutral pH and precipitates as $FeO_x(OH)_y$ (Chandra and Gerson, 2010; Singer and Stumm, 1970). Fe(oxy)hydroxides are important scavenging agents, and can reduce leachate concentrations of a number of elements (Braunschweig et al., 2013).

Only about 0.001% of V was released in both treatments, and aqueous concentrations were below 2 μg L^{-1} (Fig. 3 e). In total, 38% more leached in the DRY treatment compared to the WET ($p = 0.00002$), making it one of the elements with the greatest difference between treatments. Aqueous concentrations of V were clearly highest in the first cycle, but for the DRY treatment the leaching seemed to speed up from cycle 2 to 6, indicating that V was present in a phase sensitive to the drying period. V can occur as a contaminant in pyrite (Mindat.org, 2019). Solubility of V can be limited by scavenging by $FeO_x(OH)_y$, thus, pyrite oxidation can both increase and decrease V concentrations.

For Mo, there was a clear difference between the two treatments (Fig. 3 f). While leaching slowed from cycle 2 to 6 in the WET treatment, it stayed the same in the DRY treatment. In total 28% more leached in that treatment ($p < 0.0001$). Thus, Mo is likely also released from a phase that is sensitive to the drying period.

Leaching curves for Mn (Fig. S8) were very similar to those for the lighter alkaline earth metals (Mg, Ca and Sr, see Fig. 3 b), likely because it is often present as a bivalent ion and is a common impurity in calcite (Appelo and Postma, 2010; Rayner-Canham and Overton, 2006). The concentrations reached about 1.5 mg L^{-1} in the first cycle, and 0.15–0.4 mg L^{-1} in the rest of the cycles. As seen for Mg, Ca and Sr, Mn was released quicker in the DRY than in the WET treatment in cycles 2-6, but the overall difference between the treatments was rather small with 4% greater release in the DRY treatment ($p = 0.01$).

Cd concentrations peaked after 1 week in the first cycle at close to 45 μg L^{-1} in both treatments (Fig. 3 g) after which the concentrations decreased. In the following cycles, the Cd concentrations reached about 3–7 μg L^{-1}, with only small differences between the two treatments and slightly lower concentrations for each cycle. Very similar leaching behaviour was observed for Co, Ni and Zn (Figs. S9–S11), though at much higher concentrations of Ni and Zn, and lower of Co. Ni peaked at almost 800 μg L^{-1} in the first cycle, and in the following cycles the highest measured concentration decreased from ~110 μg L^{-1} in cycle 2–~40 μg L^{-1} in cycle 6. Zn peaked at about 500 μg L^{-1} in the first cycle and reached 40-140 μg L^{-1} in the following cycles, while for Co these numbers were about 26 μg L^{-1} and 2-5 μg L^{-1}, respectively. Of these four elements, Cd exhibited the greatest difference between the treatments with totally 10% greater leaching in the DRY treatment. While this difference was significant ($p = 0.002$), it seemed to be unrelated to the drying period of the rock, as most of it was caused by the shorter first cycle for the DRY treatment, and, thus, less reduction in concentrations. Similar statements can be made about the differences for Co, Ni and Zn displayed in Table 4.

3.3.4. Group 15

Concentrations of As were very low, with maximum concentrations below 0.6 μg L^{-1} in the first cycle and lower concentrations in the following cycles (Fig. S12). While leaching rates were higher in the DRY treatment compared to the WET treatment for the last three cycles, indicating that the drying period had an effect on the release of As, the total mass leached in the two treatments was the same. When leaching black shale, Yu et al. (2014) observed low leaching of As long as pH was above 3, and up to 1000 μg L^{-1} As in the leachate at lower pH values. Thus, we could likely have expected increased leaching of As if the system had reached low pH values.

The total mass of Sb that leached in the duration of the experiments was 24% lower in DRY compared to WET ($p = 6 \times 10^{-6}$). In cycles 2 and 3, concentrations in WET increased faster than in DRY, possibly because of limited scavenging by $FeO_x(OH)_y$ due to less pyrite oxidation. In the later cycles, the leaching rate was the same in the two treatments, but the longer contact time caused greater release in WET compared to DRY (Fig. 3 h).

3.3.5. Uranium

The total leached mass of U was 29% lower in the DRY compared to the WET treatment ($p = 0.0001$). This difference seemed to be caused only by the different contact time between debris and leachant in the two treatments, as the leaching curves followed each other in all cycles (Fig. 3 i). Thus, leaching of U seemed to not at all be affected by the drying periods. Uranium speciation in the environment strongly depends on pH and redox conditions. U in rocks is often present as the insoluble U (IV), but is easily oxidized to water-soluble U (VI) (Alloway, 2013; Landa, 2007). Since both treatments have oxidising conditions, the limiting factor for U solubility seems to be contact time and not oxidation rate.

3.3.6. Fractionation

From the measured dissolved (<0.45 μm) and low molecular mass (LMM, <10 kDa) fractions, the colloidal fraction (= dissolved – LMM) can be calculated. Colloids in the leachates can for example be newly formed precipitation products or results from flocculation and scavenging by Fe. The 10 kDa limit for colloids is an operational limit and not representing an abrupt change in actual speciation – colloids and pseudo-colloids of similar composition can occur also beneath the 10 kDa limit (Salbu, 2000). Of the elements measured in the leachates, most were present as 95-100% LMM species. S, K, Ca, As, Sr, Mo, Cd and Ba seemed to have a minor colloidal fraction, sometimes up to 10% of the dissolved element concentration. The LMM fraction of ^{226}Ra was only measured in a few time points (end of cycles 3-6 for WET and 4-6 for DRY) but indicated that ^{226}Ra as expected mainly was present as LMM species. U, on the other hand, had up to 90% colloidal fraction at the beginning of the cycles, though <10% in the end of the cycles (Fig. 4). This cyclic variation can mainly be ascribed to lower dissolved concentrations of ^{238}U in the leachate in the beginning of the cycles, but there was also a decreasing trend in calculated colloidal concentrations in each cycle with 1–3 μg L^{-1} in the beginning of a cycle and about 0.5 μg L^{-1} later in the cycle – except in cycle 1, where calculated colloidal concentrations were up to 18 μg L^{-1}.

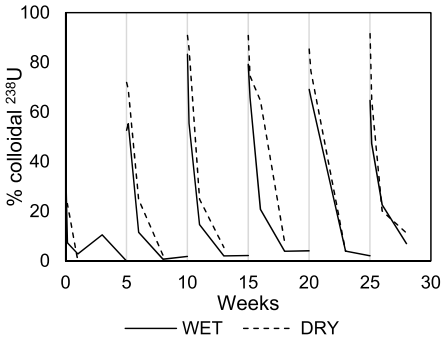

Fig. 4. Percentage colloidal fraction (<0.45 μm, >10 kDa) of ^{238}U with time in the cyclic leaching experiment.

3.4. Implications for storage of acid-producing rock

The highest release rate of the measured elements occurred in the first cycle, while in later cycles the release rate was slower. As already mentioned, this can be an artefact caused by crushing of the rock that creates very reactive fresh surfaces. These findings suggest that if rock masses are stored in water, there will be an initial release of a range of elements in high concentrations. Then, lower release rates can be expected – at least until the buffer capacity is exhausted and ARD develops.

Leaching experiments with other Scandinavian alum shales have resulted in pH levels down to 2-3 (e.g. Falk et al., 2006; Jeng, 1991; Yu et al., 2014). In the long term, a pH drop is also expected for the alum shale from Gran in the conditions tested in this experiment, as pyrite content was basically unchanged while the buffer capacity was >50% depleted. The original AP to NP ratio of 0.18 also illustrates this. Based on the observed release of S and measured TIC in the debris after treatments, new estimates for NP:AP are 0.08 and 0.09 for the debris from the WET and DRY treatment, respectively. The slightly lower estimate for WET reflects that while the pyrite oxidation (approximated by the S release) seemed to be slower in this treatment, the reduction in buffer capacity was about the same, due to the exchange of water. Thus, when the buffer capacity eventually is depleted, more pyrite is expected to be left in the WET treatment, giving a higher resulting potential for acid production.

As mentioned, rock with NP:AP > 3 is considered neutralizing (Pabst et al., 2016). However, depending on local practice and regulations, a smaller uncertainty zone can be used, and some places rocks with NP:AP > 1.2 are considered safe (Dold, 2017). For calculating the NP, the measured carbonates were all assumed to be calcite – which fits well to the XRD results in this case – and each mole of calcite were expected to neutralize 2 mol of protons (Lawrence and Wang, 1996; Pabst et al., 2016). However, because the pK_{a1} for carbonic acid is 6.3, the pH will be below 6.3 when all carbonates are spent for neutralization – which is often lower than the optimal pH in a disposal site (Dold, 2017). Thus, Dold (2017) argues that when calculating NP, only 1 mol of protons should be assumed neutralized per mole of calcite. Using this assumption, estimated NP to AP ratio of the alum shale starting material used in this experiment is 0.09. This rock debris is considered clearly acid producing in either case, but if dealing with rock masses close to being considered safe (and especially if 1.2 is used as the "safe" ratio for NP:AP), this difference in calculations can be crucial. It should be noted that another consequence of protonating HCO_3^- at low pH is outgassing of the greenhouse gas CO_2 from the disposal site.

If there is any exchange of water in a disposal site, dissolved carbonates can be transported out and buffer capacity is lost, as was seen when exchanging the water in both treatments. This means that a large fraction of the assumed buffer capacity of calcite can be lost without contributing to neutralization of acid. Thus, these results clearly show that if a disposal site is not completely sealed, the effective NP of the rock masses can be lower than expected, supporting Dold (2017) arguments for using 1 mol of H^+ per mole of calcite for NP:AP calculations. The issues with washing out of buffer capacity should also be kept in mind if a storage solution with addition of neutralizing material is chosen: if the site is not properly sealed the added buffer capacity may be washed out.

Fe and Al, major components of the debris, were not found in the leachates. As mentioned, Fe released in the pyrite oxidation will by the pH and redox conditions of the experiment precipitate as $FeO_x(OH)_y$ (Appelo and Postma, 2010; Chandra and Gerson, 2010; Grundl et al., 2011). If pH is reduced, Fe^{3+} becomes soluble and the scavenging effect of the $FeO_x(OH)_y$ ceases. Furthermore, elements previously removed

from solution can be released again causing a plume of contaminants, and the presence of Fe^{3+} in solution will accelerate the pyrite oxidation (Chandra and Gerson, 2010; Singer and Stumm, 1970). Muscovite, which likely contains all of the Al in the sample, is expected to be stable under the observed conditions, but weathering of this mineral and concomitant great release of Al is expected at lower pH values (Appelo and Postma, 2010; Hindar, 2010). Thus when a pH drop happens, considerably greater leaching of Al and Fe, together with a range of trace elements, is expected, with potentially detrimental effects on the local environment (Hindar, 2010; Rosseland et al., 1990).

The results demonstrate that the alum shale from Gran is somewhat resistant towards a pH drop, and even with drying periods and exchange of water the buffer capacity was not depleted after 28 weeks. This was also observed in previous leaching results with alum shale from this area (Fjermestad et al., 2017; Hjulstad, 2015; Wærsted, 2019), and makes the establishment of a storage site easier as there is some time to establish desirable conditions before a pH drop. On the other hand, the results clearly show that a drop in pH can be expected if oxygen is available and especially if water is exchanged, and rock debris of this type should be properly stored and precautions for avoiding oxidation should be made.

The two measured radionuclides, ^{226}Ra and ^{238}U, exhibited quite different leaching behaviour. ^{238}U was the more mobile of the two and concentrations seemed to be limited by contact time, giving higher leaching in the WET treatment. It may be desirable to maintain reducing conditions in a disposal site as avoiding oxidation of U(IV) to U(VI), would severely limit U mobility. The exchange of water seemed to greatly increase leaching of ^{226}Ra by reducing the scavenging by $BaSO_4$. Thus, in a disposal site, mobility of ^{226}Ra can be expected to drastically increase if water is exchanged. While one could argue that oxidising conditions are good for limiting mobility of Ra, due to the high sulphate concentrations, the negative environmental effects by developing ARD and increasing mobility of many other trace elements are likely to be much greater.

4. Conclusions

The effect of water exchange and drying periods on the leaching of alum shale was investigated. Most measured elements leached the greatest amount in the first cycle – the first contact with water – giving neutral rock drainage. Thus, when alum shale debris comes in contact with water, an initial high release of contaminants can be expected, then leaching rates are expected to decrease for most elements until an eventual pH drop and onset of ARD that is likely to increase leaching and solubility for a range of elements. This also means that a high leaching rate of a range of elements can be expected on an excavation site if the debris is not immediately moved to a disposal site or protected from flowing water. Some elements showed continued leaching in cycle after cycle, especially Ba, ^{226}Ra, Sb, V and Mo, though Ba was the only element that reached similar concentrations in later cycles as in the first.

Higher concentrations of SO_4^{2-}, conductivity and lower alkalinity indicated a greater extent of oxidation of sulphides in debris that was allowed to dry in air between leaching cycles (DRY) compared to the debris kept submerged in water at all times (WET). However, the differences were rather small, and for some elements the longer contact time with water in WET compensated for the higher leaching rates in DRY, and the resulting total leached masses were the same. Increased leaching of several investigated elements, most clearly for Li, V, Mo, SO_4 and ^{226}Ra, was observed after periods when the rock debris was exposed directly to air and allowed to dry. Sb and ^{238}U leached more in the WET treatment compared to the DRY. For ^{238}U, the only factor of importance for the leaching seemed to be the contact time between debris and leachant.

The results from these experiments clearly demonstrate the challenges of storing alum shale or other acid-producing rock in water that is not completely stagnant. Exchange of water not only causes oxygenated water to enter and contaminated water to leak out, but can also increase leaching of elements which are limited by solubility (like Ba and ^{226}Ra) and wash out important buffer capacity in the form of dissolved carbonates. Washing out the inherent buffer capacity of the stored rock masses can increase risk of ARD and reduce time before onset of ARD. Thus, exchange of the water in a storage site decreases the buffer capacity of the debris (reduces the carbonates) – with or without oxygen coming in – and rocks masses that were assumed to be neutralizing can turn into acid-producing as the NP:AP changes.

While the treatment with drying periods resulted in greater leaching in the duration of the experiment, the treatment with exchange of water without drying seemed to result in slightly lower NP:AP values at the end of the experiment, and, thus, in debris with an even greater potential for ARD. Despite the slight differences, neither of the tested treatments are recommended for storage of alum shale or other acid-producing rock: if such rock is stored in water, exchange of water and intrusion of air should be kept at an absolute minimum.

Declaration of competing interest

The authors declare that they have no known competing financial interests or personal relationships that could have appeared to influence the work reported in this paper.

Acknowledgements

This study has been funded by the Norwegian Public Road Administration through the NORWAT (Nordic Road Water) programme and by the Norwegian Research Council through its Centre of Excellence (CoE) funding scheme (Project 223268/F50).

Appendix A. Supplementary data

Supplementary data to this article can be found online at https://doi.org/10.1016/j.apgeochem.2020.104610.

References

Aas, W., Platt, S., Solberg, S., Yttri, K.E., 2015. Monitoring of Long-Range Transported Air Pollutants in Norway, Annual Report 2014 (M-367).
Alloway, B.J., 2013. In: Alloway, B.J., Trevors, J.T. (Eds.), Heavy Metals in Soils: Trace Metals and Metalloids in Soils and Their Bioavailability, third ed. Springer.
Appelo, C.A.J., Postma, D., 2010. Geochemistry, Groundwater and Pollution, second ed. CRC press.
Braunschweig, J., Bosch, J., Meckenstock, R.U., 2013. Iron oxide nanoparticles in geomicrobiology: from biogeochemistry to bioremediation. N. Biotech. 30 (6), 793–802. https://doi.org/10.1016/j.nbt.2013.03.008.
Chandra, A.P., Gerson, A.R., 2010. The mechanisms of pyrite oxidation and leaching: a fundamental perspective. Surf. Sci. Rep. 65 (9), 293–315. https://doi.org/10.1016/j.surfrep.2010.08.003.
CRC Handbook of Chemistry and Physics. (1993). (D. R. Lide Ed., 74th ed.). U.S.A.: CRC.
Dold, B., 2017. Acid rock drainage prediction: a critical review. J. Geochem. Explor. 172, 120–132. https://doi.org/10.1016/j.gexplo.2016.09.014.
Endre, E., 2013. *Identifisering Og Karakterisering Av Skiferhorisonter I Tunneltraséen* (20120110-R=1). Norwegian Geotechnical Institute.
Endre, E., Sørmo, E., 2015. In: Institute, N.G. (Ed.), Identifisering Og Karakterisering Av Syredannende Bergarter: Veileder for Miljødirektoratet M-310 (M-310) (miljodirektoratet.no:).
Falk, H., Lavergren, U., Bergbäck, B., 2006. Metal mobility in alum shale from Öland, Sweden. J. Geochem. Explor. 90 (3), 157–165. https://doi.org/10.1016/j.gexplo.2005.10.001.
Fjermestad, H., Gundersen, E., Hagelia, P., Moen, A.B., Torp, M., 2018. National Road 4, utilization of black shale - final report and experiences gathered (333). Retrieved from. www.vegvesen.no/.
Fjermestad, H., Hagelia, P., Thomassen, T., 2017. Large-scale leaching experiment with black shale from National Road 4, Hadeland (665). Retrieved from. www.vegvesen.no.
Gabitov, R.I., Gagnon, A.C., Guan, Y., Eiler, J.M., Adkins, J.F., 2013. Accurate Mg/Ca, Sr/Ca, and Ba/Ca ratio measurements in carbonates by SIMS and NanoSIMS and an assessment of heterogeneity in common calcium carbonate standards. Chem. Geol. 356, 94–108. https://doi.org/10.1016/j.chemgeo.2013.07.019.
Grundl, T.J., Haderlein, S., Nurmi, J.T., Tratnyek, P.G., 2011. Introduction to aquatic redox Chemistry. In: Aquatic Redox Chemistry, vol. 1071. American Chemical Society, pp. 1–14.

Hindar, A., 2010. Highway E18 Grimstad-Kristiansand; Effects and Quantification of Acid Runoff from Deposits of Sulphide-Bearing Rock. Retrieved from. http://brage.bibsys.no.

Hjulstad, M., 2015. Leaching, Uptake and Effects in Brown Trout (Salmo trutta) of Radionuclides and Metals from Black Shales and Sulphur Bearing Gneiss (MSc). Norwegian University of Life Sciences, Ås, Norway.

Jeng, A.S., 1991. Weathering of Some Norwegian Alum Shales. I. Laboratory simulations to study acid generation and the release of sulfate and metal cations (calcium, magnesium, and potassium). Acta Agric. Scand. 41 (1), 13–35. https://doi.org/10.1080/00015129109438580.

Jeng, A.S., 1992. Weathering of some Norwegian alum shales, II. Laboratory simulations to study the influence of aging, acidification and liming on heavy metal release. Acta Agric. Scand. Sect. B Soil Plant Sci 42 (2), 76–87. https://doi.org/10.1080/09064719209410203.

Kirby, H.W., Salutsky, M.L., 1964. The Radiochemistry of Radium (NAS-NS 3057).

Landa, E.R., 2007. Naturally occurring radionuclides from industrial sources: characteristics and fate in the environment. In: George, S. (Ed.), Radioactivity in the Environment, vol. 10. Elsevier, pp. 211–237.

Lavergren, U., Åström, M.E., Falk, H., Bergbäck, B., 2009. Metal dispersion in groundwater in an area with natural and processed black shale – nationwide perspective and comparison with acid sulfate soils. Appl. Geochem. 24 (3), 359–369. https://doi.org/10.1016/j.apgeochem.2008.11.022.

Lawrence, R.W., Scheske, M., 1997. A method to calculate the neutralization potential of mining wastes. Environ. Geol. 32 (2), 100–106. https://doi.org/10.1007/s002540050198.

Lawrence, R.W., Wang, Y., 1996. Determination of neutralization potential for acid rock drainage prediction (MEND project 1.16.3). Retrieved from. http://mend-nedem.org/mend-report/determination-of-neutralization-potential-for-acid-rock-drainage-prediction/.

Miller, J.N., Miller, J.C., 2005. Statistics and Chemometrics for Analytical Chemistry. Pearson Education Limited, Great Britain.

Mindatorg, 2019. Pyrite. Retrieved from. https://www.mindat.org/min-3314.html on 22. (Accessed June 2019).

Owen, A.W., Bruton, D.L., Bockelie, J.F., Bockelie, T.G., 1990. The ordovician successions of the Oslo region, Norway. In: Roberts, D. (Ed.), Geological Survey of Norway (NGU). Retrieved from. http://paleoarchive.com/.

Pabst, T., Sørmo, E., Endre, E., 2016. Geochemical characterisation of Norwegian Cambro-Ordovician black mudrocks for building and construction use. Bull. Eng. Geol. Environ. 76 (4), 1577–1592. https://doi.org/10.1007/s10064-016-0941-z.

Parbhakar-Fox, A., Lottermoser, B.G., 2015. A critical review of acid rock drainage prediction methods and practices. Miner. Eng. 82, 107–124. https://doi.org/10.1016/j.mineng.2015.03.015.

Pipkin, B., Trent, D.D., Hazlett, R., Bierman, P., 2008. In: Adams, P. (Ed.), Geology and the Environment, fifth ed. Thomson Brooks/Cole, USA.

Pollution Control Act (Forurensningsforskriften), FOR-2004-06-01-931 (2004).

Rayner-Canham, G., Overton, T., 2006. In: Fiorillo, J. (Ed.), Descriptive Inorganic Chemistry, fourth ed. W. H. Freeman and Company, Houndmills, England.

Rosseland, B.O., Eldhuset, T.D., Staurnes, M., 1990. Environmental effects of aluminium. Environ. Geochem. Health 12 (1–2), 17–27. https://doi.org/10.1007/bf01734045.

Salbu, B., 2000. Speciation of radionuclides in the environment. In: Meyers, R.A. (Ed.), Encyclopedia of Analytical Chemistry. John Wiley & Sons Ltd, Chichester, pp. 12993–13016.

Sima, M., Dold, B., Frei, L., Senila, M., Balteanu, D., Zobrist, J., 2011. Sulfide oxidation and acid mine drainage formation within two active tailings impoundments in the Golden Quadrangle of the Apuseni Mountains, Romania. J. Hazard Mater. 189 (3), 624–639. https://doi.org/10.1016/j.jhazmat.2011.01.069.

Singer, P.C., Stumm, W., 1970. Acidic mine drainage: the rate-determining step. Science 167 (3921), 1121–1123. https://doi.org/10.2307/1728684.

Sørmo, E., Breedveld, G., Pabst, T., 2015. Deponering Av Syredannende Bergarter. Grunnlag for Veileder. (M-385).

Stegnar, P., Shishkov, I., Burkitbayev, M., Tolongutov, B., Yunusov, M., Radyuk, R., Salbu, B., 2013. Assessment of the radiological impact of gamma and radon dose rates at former U mining sites in Central Asia. J. Environ. Radioact. 123, 3–13. https://doi.org/10.1016/j.jenvrad.2012.12.005.

Strålevernforskriften, 2016. Forskrift om strålevern og bruk av stråling, FOR-2016-12-16-1659.

vanLoon, G.W., Duffy, S.J., 2011. Environmental Chemistry - a Global Perspective, third ed. Oxford University Press, New York.

Wærsted, F.M., 2019. Mobility Of Naturally Occurring Radionuclides and Stable Elements in Alum Shale: A Case Study of Gran, Highway 4, Norway (PhD). Norwegian University of Life Sciences. https://hdl.handle.net/11250/2651558.(2019:72).

Wærsted, F.M., Jensen, K.A., Reinoso-Maset, E., Skipperud, L., 2018. High throughput, direct determination of 226Ra in water and digested geological samples. Anal. Chem. 90 (20), 12246–12252. https://doi.org/10.1021/acs.analchem.8b03494.

Yu, C., Lavergren, U., Peltola, P., Drake, H., Bergbäck, B., Åström, M.E., 2014. Retention and transport of arsenic, uranium and nickel in a black shale setting revealed by a long-term humidity cell test and sequential chemical extractions. Chem. Geol. 363, 134–144. https://doi.org/10.1016/j.chemgeo.2013.11.003.